Regulation of the flavin redox potential by flavin-binding antibodies

European Journal of Biochemistry

Bruggeman, Y.E.; Honegger, A.; Kreuvel, H.; Visser, A.J.W.G.; Laane, C. et al

https://doi.org/10.1111/j.1432-1033.1997.00393.x

Eur. J. Biochem. 249, 393–400 (1997)

Regulation of the flavin redox potential by flavin-binding antibodies

Yvonne E. BRUGGEMAN[1], Annemarie HONEGGER[2], Huub KREUWEL[1], Antonie J. W. G. VISSER[1], Colja LAANE[1], Arjen SCHOTS[3] and Riet HILHORST[1]

[1] Laboratory for Biochemistry, Agricultural University Wageningen, The Netherlands
[2] Biochemisches Institut der Universität Zürich, Zürich, Switzerland
[3] Laboratory for Nematology – Antibody Technology Section, Agricultural University Wageningen, The Netherlands

(Received 16 May/15 August 1997) – EJB 97 0694/3

Single-chain Fv antibody fragments binding different flavin forms [10-(5′-carboxybutyl-)flavin (Fl_{ox}) and 10-(5′-carboxybutyl)-1,5-dihydroflavin (Fl_{red})] have been generated from an antibody phage-display library to study how a protein environment regulates the redox potential, starting from a protein other than a natural flavoprotein. These 'flavobodies' are characterized by time-resolved and steady-state fluorescence spectroscopy, by competitive ELISA methods (mapping of the antigen-binding site), and by molecular modelling. The three-dimensional models of the antigen-binding sites are consistent with the experimental results. Binding of anti-Fl_{red} 5 to flavin increases the redox potential, mainly due to an Arg residue interacting with the flavin N1. Thus anti-Fl_{red} 5 shows an 'oxidase-like' redox-potential behaviour, confirming the idea that positively charged residues in the vicinity of N1 increase the redox potential. The results obtained with anti-Fl_{ox}, which do not resemble a natural flavoprotein, show that when the pyrimidine-like nucleus of the flavin is not involved in binding, the redox potential is not significantly affected. These results are in contrast to those obtained with chicken riboflavin-binding protein.

Keywords: flavin; flavoprotein oxidase; antibody-binding domain; modeling; phage display.

Flavin acts as cofactor in many redox enzymes and electron-transferring proteins. These flavin-containing enzymes catalyse a wide variety of biochemical reactions varying from oxidase-type to dehydrogenase-type and monooxygenase-type of reactions. This versatility sets flavoproteins apart from most other cofactor-dependent enzymes which, in general, only catalyse a single type of reaction (Ghisla and Massey, 1989). The redox-active part of the flavin is the isoalloxazine ring, which can exist in oxidized flavoquinone, one-electron-reduced flavosemiquinone and two-electron-reduced flavohydroquinone states. The flavin redox potentials depend on the nature of the active site in which the flavin resides and vary largely among different flavoproteins (Stankovich, 1990). The role of the protein environment of the flavin cofactor in modulating the redox potential is still not properly understood. Here we have investigated the structural and redox properties of monoclonal antibodies elicited against oxidised and two-electron-reduced flavin and compared them with those of 'natural' flavoproteins.

The isoalloxazine moiety of the flavin is amphipatic, consisting of a hydrophobic benzene-like part (ring A) and a hydrophilic pyrimidine moiety (ring C; Fig. 1). The N5 atom in ring B is electron deficient and is the site where the electrons enter the isoalloxazine (Platenkamp et al., 1987). The negative charge is spread over C4a, N5, N10 and N1 (Hall et al., 1987b). The degree to which this negative charge is stabilised or destabilised is an important factor governing the redox potential: a positive charge in the protein around ring C will contribute to increase the redox potential, whereas a negatively charged or hydrophobic environment will decrease it. This is clearly shown in the X-ray structures of several flavoprotein oxidases: glycolate oxidase (Lindqvist, 1989) has a positively charged Lys residue, and glucose oxidase (Hecht et al., 1993) and cholesterol oxidase (Vrielink et al., 1991) have His residues in the vicinity of ring C, which stabilise the reduced flavin. In the one-electron-transferring flavodoxin, however, the flavin hydroquinone is destabilised by negative charges in the vicinity (within 13 Å) of the N1 atom of the flavin (Zhou and Swenson, 1995).

The apolar part of the flavin, ring A, is either in contact with bulk solvent frequently, for example in flavodoxin and cholesterol oxidase, or is bound by hydrophobic interactions as in glucose oxidase or riboflavin-binding protein (Monaco, 1997). Ring A is often not involved in the reduction and/or reoxidation of the flavin moiety and only plays an indirect role by serving as polarisable source for the changes occurring in the redox-active N1-C10a-C4a-N5 region, in that way fine tuning the modulation of the redox potential (Hall, 1987).

These findings illustrate that the environment of ring C mainly regulates the redox potential, suggesting that a protein only binding to ring A should hardly influence the redox potential. Monoclonal antibodies, or even antibody fragments consisting of the two variable (V) antigen-binding domains, offer a way to build artificial protein environments specific for different flavin redox states (Bruggeman et al., 1995, 1996; Shokat et al., 1988). This is possible because oxidized flavin differs from reduced flavin in its conformational and electronic properties. It might even be possible to generate 'unnatural' flavin-binding proteins that recognize both redox states equally well (i.e. the redox potential is not influenced) by generating antibodies that bind to ring A.

Correspondence to R. Hilhorst, Laboratory for Biochemistry, Dreijenlaan 3, NL-6703 HA Wageningen, The Netherlands
Fax: +31 317 484801.
E-mail: riet.hilhorst@laser.bc.wau.nl

Abbreviations. CDR, complementarity-determining region; Fl_{ox}, 10-(5′-carboxybutyl-)flavin; Fl_{red}, 10-(5′-carboxybutyl)-1,5-dihydroflavin; V domain, antibody variable domain; E'_0, redox potential; H chain, heavy chain; L chain, light chain.

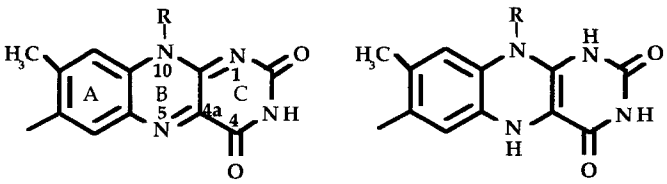

flavin 1,5-dihydroflavin

	R
Flox	$(CH_2)_4$-COOH
riboflavin	ribityl
FMN	ribityl-phosphate

Fig. 1. Structures of flavin analogues used.

To contribute to a better understanding of how the protein environment regulates the flavin redox potential, we have generated single-chain Fv antibody fragments [composed of the two antigen-binding domains connected by a peptide linker (Bird, 1988)] against reduced (Bruggeman et al., 1996) and oxidized flavin from a naive antibody phage-display library (Nissim et al., 1994). (In such a library an antibody repertoire is cloned on the surface of filamentous bacteriophage, and antibodies can be selected by panning the library on antigen.) Here we show that an antibody fragment binding mainly to ring A of 10-(5′-carboxybutyl-)flavin (Fl_{ox}) does not influence the flavin redox potential (E_0') significantly, whereas an antibody fragment binding ring C of 10-(5′-carboxybutyl)-1,5-dihydroflavin (Fl_{red}) causes a shift in E_0' of +65 mV.

EXPERIMENTAL PROCEDURES

Phage selection. A 'single pot' human synthetic phage-antibody single-chain Fv library (Nissim et al., 1994) was used for phage selection. Phage were selected for binding to Fl_{ox} (Bruggeman et al., 1996) as described by Nissim et al. (1994) and eluted with 100 mM Fl_{ox} in 0.15 mM NaCl, 0.1 M P_i, pH 7.2. Clones found to give a positive ELISA signal were screened by PCR and 'fingerprinted' by the frequent-cutting restriction enzyme *Bst*NI as described by Marks et al. (1991) to identify different clones. Examples of clones with different restriction patterns were selected and the 3′ ends of the heavy (H) chains were sequenced to confirm the fingerprinting as described by Bruggeman et al. (1996).

The selection of a phage antibody (anti-Fl_{red} 5) against the Fl_{red} has been described previously (Bruggeman et al., 1996).

Expression, purification and sequence analysis. For soluble expression, selected clones were subcloned into pUC119SfiNotMycHis [lacking the gene III insert but harbouring a hexahistidine tag for purification and a c-Myc tag (Munro and Pelham, 1986) for detection] using standard recombinant DNA techniques. A 1-l culture of *E. coli* TG1 harbouring each plasmid was grown to an A_{600} of 0.9 and single-chain Fv expression was induced with isopropylthio-β-galactoside (De Bellis and Schwartz, 1990). After induction, the culture was shaken for 3 h at 20°C. Since no single-chain Fv could be detected in the culture supernatant, single-chain Fv was purified from the cells. Cells were suspended in 50 mM sodium phosphate, pH 7.5, 500 mM NaCl, 20 mM imidazole and 2 mM phenylmethylsulfonyl fluoride and lysed by two passes through a French pressure cell at 124 MPa. Cell walls and insoluble material were removed from the lysate by centrifugation at 28000×*g* for 30 min. The single-chain Fv was purified by immobilized metal-affinity chromatography (Hochuli et al., 1987) as described by Griffiths et al. (1994). All purification steps were performed at 4°C. Purified single-chain Fv fragments were judged for purity by SDS/PAGE. The single-chain Fv concentration was determined spectrophotometrically using ε_{280} values determined from the amino acid sequences as described in Gill and von Hippel (1989).

For sequencing, DNA purified with Qiagen Plasmid Midiprep (Qiagen Inc.) was subjected to PCR cycle-sequencing reactions with fluorescent dideoxynucleotide chain terminators (Applied Biosystems) according to the manufacturer's instructions using standard M13 primers. The sequencing reactions were analysed on an Applied Biosystems 373 automated DNA sequencer. Sequence analysis was performed using AutoAssembler (Applied Biosystems).

Mapping of the antigen-binding site with flavin analogues. Competitive ELISA was used to study binding of anti-Fl_{ox} to Fl_{ox}, FMN (Boehringer Mannheim) and riboflavin (Sigma) in 0.15 M NaCl, 0.1 M P_i, pH 7.2. Basically, the method described by Friguet et al. (1985) was followed (omitting the preincubation step).

Binding of anti-Fl_{ox} to Fl_{ox} and Fl_{red} was compared using time-resolved polarized fluorescence as described in Bruggeman et al. (1995). Fl_{ox} and Fl_{red} were excited with light of 450 nm. Flavin was titrated with varying antibody concentrations.

Steady-state fluorescence was used to investigate binding of anti-Fl_{ox} to Fl_{ox}, riboflavin and FMN. 0.2−0.7 μM anti-Fl_{ox} was titrated with flavin up to 10 μM. Emission spectra (300−350 nm) were recorded after exciting at 280 nm on a SPF 500C Spectrofluorometer (SLM Aminco). Excitation and emission monochromator bandwidths were set at 4 nm.

Binding of anti-Fl_{red} 5 to Fl_{ox} and Fl_{red} was studied with time-resolved fluorescence and to Fl_{ox} and riboflavin using competitive ELISA as described previously (Bruggeman et al., 1996).

Computer modeling of the antigen-binding site. Structural models of the variable domains of the heavy and light chains (V_H and V_L) of anti-Fl_{ox} and anti-Fl_{red} 5 were derived by homology modeling based on sequence similarity with antibody structures from the Brookhaven protein database (PDB; Bernstein et al., 1977). We used the Unix Insight II package (version 2.3.0), including the modules Biopolymer and Homology, and Discover (version 94.0) from Biosym/MSI. The amino acid sequences of the variable domains of the antibodies have been used as program input for the modeling of three-dimensional structures.

The λ V_L domain is the same in both single-chain Fv fragments (Nissim et al., 1994). The best templates for this V_L domain were the V_L domain of antibody HIL (PDB entry 8fab, 1.8-Å resolution) with 66.7% sequence identity, the MCG light-chain dimer (3mcg, 2.0 Å resolution) with 62.7% sequence identity, and the V_L domain of antibody KOL (2ig2, 1.9-Å resolution, and 2fb4, 3.0-Å resolution) with 58.7% sequence identity. After structural alignment of the four potential template structures and careful analysis of the influence of local sequence differences on the structures of the potential template molecules, the majority of the coordinates were assigned using 8fab as a template. The third complementarity-determining region (CDR3), which in λ chains shows much higher structural variability than in κ chains, was modelled based on the coordinates of 2ig2.

The best templates for the V_H domain of anti-Fl_{red} 5 were the V_H domains of the antibody 3D6 (1dfb, 2.7-Å resolution) with 73.6% sequence identity, followed by antibody POT (1igm, 2.3-Å resolution) with 72.5% identity, and HIL (8fab, 1.8-Å resolution) with 70.6% sequence identity. 1dfb was used as primary template for the modeling of the V_H domain. The CDR3 of PDB entries 1fvw, 2fvw, 8fab, 1igm and 6fab all have the same length as that of anti-Fl_{red} 5, but these antibodies have a salt bridge

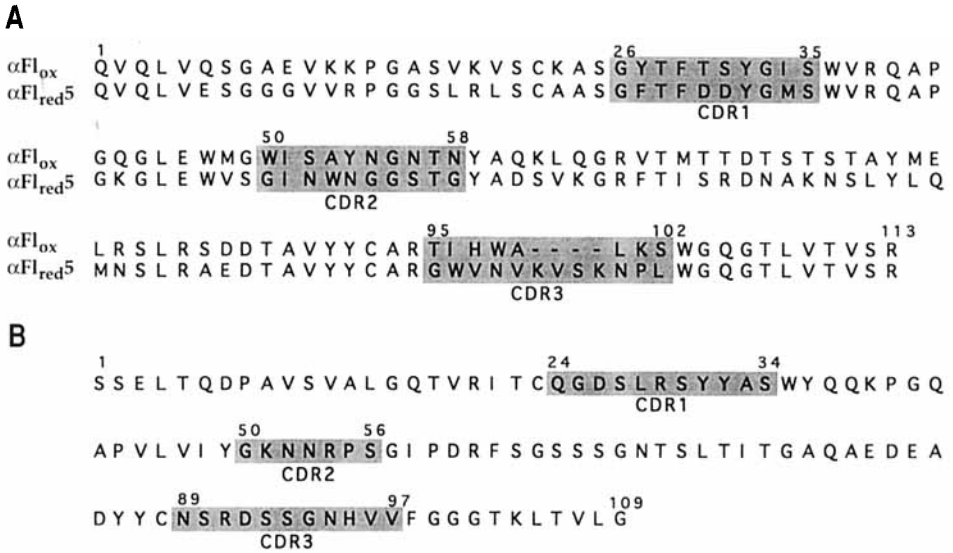

Fig. 2. Amino acid sequences of anti-Fl_{ox} (αFl_{ox}) and anti-Fl_{red} 5 (αFl_{red} 5) heavy-chain (A) and light-chain (B) domains. The light chain is the same in both antibodies. CDR are shaded. Numbering is according to Kabat et al. (1992).

between ArgH94 and AspH101 (Chothia and Lesk, 1987), which strongly influences the conformation of CDR3, while anti-Fl_{red} 5 lacks this salt bridge. Therefore CDR3 was modelled using 2fvb as a template, shortening the loop by two residues. The lack of the Arg-Asp salt bridge suggests an 'open' conformation of this CDR3, in which the loop sticks out into the solvent and is highly flexible.

For the V_H domain of anti-Fl_{ox}, the best templates were the antibody DB3 (2dbl, 2.9 Å, and 1dba, 1dbb, 1dbj, 1dbk, 1dbm) with 54.2% sequence identity (but a higher similarity score than the others), followed by antibodies TE33 (1tet, 2.3 Å) with 56% sequence identity, and R19.9 (1fai, 2.7 Å) with 58.7% sequence identity. The model was based primarily on the structure of 2dbl. Analogous to anti-Fl_{red} 5, anti-Fl_{ox} lacks the Arg94-Asp101 salt bridge and therefore the PDB entries 1vfa, 1fdl and 1mam, which have CDR3 of similar length, could not be used as templates. Here CDR3 was modelled by extending the CDR3 of 1baf by two amino acids.

The relative orientation of the V_H and V_L domains was determined by structural alignment with the F_V fragments of the primary templates. After conjugate gradient energy minimization of the models, the ligands (Fl_{ox} and Fl_{red}) were docked manually and the complexes were annealed in a 20-ps molecular-dynamics run. Charges were assigned consistent with the protonation states expected at pH 7.4. The force field used was the consistent valence force field, and dynamics and minimization were performed without explicit solvent, using a distance-dependent dielectric constant.

RESULTS

Selection of phage antibodies and expression as single-chain Fv fragments. Phage antibodies against oxidized flavin (Fl_{ox}) were selected using standard selection techniques. As revealed by *Bst*NI fingerprinting and confirmed by sequencing, at least four different clones have been selected. The clone giving the best ELISA signal to Fl_{ox} (anti-Fl_{ox}) was chosen for further characterization as soluble single-chain Fv fragment. The selection of the reduced flavin-binding single-chain Fv anti-Fl_{red} 5 has been described previously (Bruggeman et al., 1996). Anti-Fl_{ox} and anti-Fl_{red} 5 were purified with yields of 1.5 mg/l and 0.6 mg/l, respectively.

Sequence analysis. The primary structures of the variable regions of both antibodies have been determined (Fig. 2). The light (L) chain is the same for both antibodies since the library we used has an unmutated light chain (IGLV3S1; Marks et al., 1991) as described by Hoogenboom and Winter (1992). The similarity in framework region 4 and the end of framework region 3 of the H chain has been imposed by the way the library was constructed (Nissim et al., 1994). Anti-Fl_{ox} comprised V_H segment DP-14 (Tomlinson et al., 1992) with an 8-amino-acid CDR3, and anti-Fl_{red} 5 comprised V_H segment DP-32 with a 12-amino-acid CDR3. Both antibodies lack the characteristic ArgH94-Asp101 salt bridge (Chothia and Lesk, 1987).

Mapping of the antigen-binding site. To determine the affinities of anti-Fl_{ox} and anti-Fl_{red} 5 for different flavins, we had to resort to a variety of techniques. Steady-state fluorescence, based on quenching of Trp fluorescence upon hapten binding, is usually the method of choice since the affinity can be determined directly in solution and the method is very sensitive. Competitive ELISA is another good approach but requires more antibody and hapten. We used both methods to study affinities for oxidized flavins. However, due to the low fluorescence quantum yield, the poor visible-light absorption, and the instability of reduced flavin in an aerobic environment, it is not possible to determine the affinities of these antibodies for two-electron-reduced flavin using these standard techniques. Because of its sensitivity, we used time-resolved fluorescence to investigate binding to reduced flavin.

Time-resolved polarized fluorescence. Binding of Fl_{ox} and Fl_{red} to anti-Fl_{ox} and anti-Fl_{red} 5 (Bruggeman et al., 1996) was studied by time-resolved polarized fluorescence.

The total fluorescence decays for free and anti-Fl_{ox}–bound Fl_{ox} and Fl_{red} are shown in Fig. 3. The fluorescence of antibody-bound Fl_{ox} (Fig. 3A) exhibits a faster decay than the fluorescence of free Fl_{ox}, indicative of binding. The fluorescence-lifetime distributions, derived from these total fluorescence decays, are consistent with these observations. Free Fl_{ox} (Fig. 3B) has a major lifetime of 4.2 ns and two smaller contributions. Upon addition of antibody the contribution of the component at 4.2 ns decreases and two lifetimes, at 0.9 ns and 0.1 ns, show up. The shortening of fluorescence lifetimes indicates a dynamic quenching process.

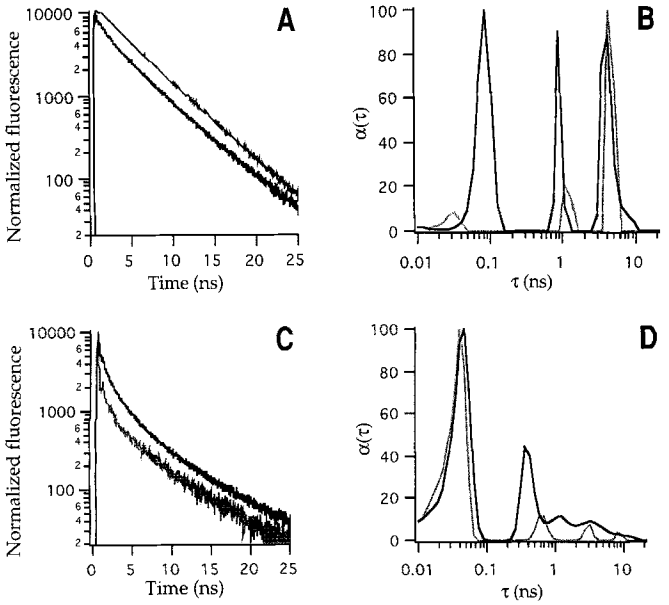

Fig. 3. Experimental total fluorescence decays and fluorescence-lifetime distributions of free and anti-Fl_{ox}–bound Fl_{ox} and Fl_{red}. Grey curves reflect free Fl_{ox} (A, B) or free Fl_{red} (C, D). Black curves reflect bound species. In all experiments the residuals of the fit were randomly scattered around zero, indicating an optimal fit.

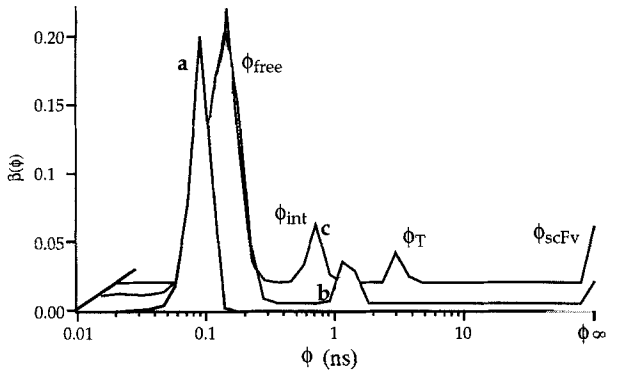

Fig. 4. Rotational-correlation-time distributions of free and anti-Fl_{ox}–bound Fl_{ox}. Curve a, free Fl_{ox}; curve b, Fl_{ox}/anti-Fl_{ox} 1:140; curve c, Fl_{ox}/anti-Fl_{ox} 1:280.

In contrast to this, the fluorescence decay of anti-Fl_{ox}–bound Fl_{red} is slower than that of free Fl_{red} (Fig. 3C). The fluorescence-lifetime-distribution patterns corresponding to these curves are more complex than those of Fl_{ox} (Fig. 3D) as a result of the presence of multiple, non-planar conformations that interconvert into each other (Visser et al., 1991). This conformational instability is the cause of the low fluorescence quantum yield of reduced flavin (Ghisla et al., 1974). The increase in fluorescence upon antibody binding, reflected in the increased contributions of longer lifetime components (including a peak at 0.6 ns), indicates a hindered ring inversion of the flavohydroquinone due to antibody binding (Ghisla et al., 1974).

We derived information about flavin motion from rotational correlation times obtained from fluorescence anisotropy decays. Whereas free Fl_{ox} shows a single rotational correlation time (ϕ_{free} = 0.2 ns) (Fig. 4), we observe two more contributions upon titration of Fl_{ox} with anti-Fl_{ox}: one due to the internal restricted motion of the flavin in the antigen-binding site (ϕ_{int} = 1 ns); and a contribution at infinite time (not resolvable) that corresponds to tumbling of the single-chain Fv ($\phi_{sc\ Fv}$). However, when more

Table 1. Summary of affinity constants (K_d) and redox potential shifts (ΔE). Samples were analysed by time-resolved fluorescence spectroscopy or ELISA, at pH 7.2 (unless indicated otherwise). n.d., not determined.

Antibody	Flavin	Analysis method	K_d	ΔE
			μM	mV
Anti-Fl_{ox}	Fl_{ox}	spectroscopy	43	+8
		ELISA	15.5	n.d.
	Fl_{red}	spectroscopy	23	n.d.
	riboflavin	ELISA	43	n.d.
	FMN	ELISA	42	n.d.
Anti-Fl_{red}	Fl_{ox}	ELISA	100	+41
	Fl_{red}	spectroscopy	4.0[a], 0.6[b]	+65[b]
	riboflavin	ELISA	>100	n.d.

[a] pH 6.0.
[b] pH 7.5.

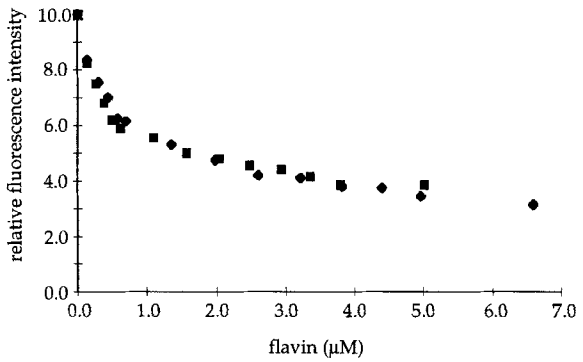

Fig. 5. Tryptophan quenching in anti-Fl_{ox}. ◆, anti-Fl_{ox}/Fl_{ox}; ■, anti-Fl_{ox}/riboflavin.

antibody is added a fourth contribution, at 2.2 ns, emerges. We ascribe this peak (ϕ_T) to homo-(energy transfer) (i.e. energy transfer between two identical flavin chromophores). This can be explained by assuming dimer formation; single-chain Fv fragments secreted from bacteria are often present as monomers and dimers (Griffiths et al., 1993), suggesting that the V_H and V_L domains of different chains can pair. The distance between the two antigen-binding sites of the dimer, i.e. the distance between the two bound flavins, can be calculated from the Förster equation as described in Bastiaens et al. (1991, 1992b), using values from Bastiaens et al. (1992a).

For the dimer form of the single-chain Fv anti-Fl_{ox} we determined a centre-to-centre distance (R) of 32 Å between the two antigen-binding sites at an angle (θ) of 143 ± 1.3°. From the crystal structure of a dimerized antibody with a five-residue flexible linker, a distance of 65 Å between the antigen-binding sites has been determined (Perisic et al., 1994). However, anti-Fl_{ox} has a 15-residue $(Gly_4Ser)_3$ linker and hence there will be less constraint between the two subunits of the dimer so that they can approach each other more closely.

The affinity constants of anti-Fl_{ox} for Fl_{ox} and Fl_{red} were calculated from the decrease of the free flavin contribution in the rotational correlation times as described by Bruggeman et al. (1996) (Table 1). The affinity constants of anti-Fl_{red} 5 for Fl_{red} (both protonated and deprotonated at N1) have been published elsewhere (Bruggeman et al., 1996) and are included in Table 1 for comparison.

Steady-state fluorescence. We investigated binding of anti-Fl_{ox} to Fl_{ox}, riboflavin and FMN using steady-state fluorescence. Fig. 5 shows the quenching of the Trp fluorescence upon titrating with Fl_{ox} and riboflavin. The titration curves show a striking biphasic pattern that could not be fitted to a function describing the hyperbolic curve characteristic for antibody-antigen binding (Bruggeman et al., 1996). The large initial decrease could not be due to photobleaching of the Trp since in the absence of flavin and under continuous excitation (for 20 min) there is only a fast 6% decrease in Trp fluorescence followed by stabilisation of the Trp emission. Moreover, the decrease was not dependent on the light intensity.

However, it has been known for a long time that flavins can sensitise the destructive photooxidation of a large variety of substrates, such as amino acids, in the presence of oxygen (Taylor and Radda, 1971). Our results indicate that one or more Trp residues in the anti-Fl_{ox}−binding site are sensitive to photooxidation, explaining the large initial fluorescence decrease in the titration curve. However, that after the breakpoint in the curve the Trp fluorescence still slowly decreases suggests that there are also Trp residues involved in binding that are not sensitive to photooxidation. Thus, the crippled antibody that remains after photooxidation is still capable of binding flavin although with a decreased affinity (reflected in the flatter part of the titration curve). Fl_{ox} and riboflavin both have the same effect on photooxidation since the titration curves overlap. Therefore it is not possible to pronounce upon differences in affinity between two flavin analogues.

The breakpoint in the titration curves is located around 0.5 μM flavin. Since it has been known that part of the purified antibody might be incorrectly folded (Knappik and Plückthun, 1995), we assume that this is the concentration of correctly folded antibody (we assume that only correctly folded antibody binds flavin). This implies that only one Trp residue is close enough to the flavin to be photooxidized since this is less than equimolar to the antibody concentration (0.7 μM). From this it can be estimated that 70% of the purified single-chain Fv has been properly folded.

We could not determine the affinity of anti-Fl_{ox} for Fl_{red} using this approach, because dithionite, used to reduce flavin, quenches the Trp fluorescence. Furthermore, we could not study binding of Fl_{ox} (and other flavin derivatives) to anti-Fl_{red} 5 due to the weak binding of this single-chain Fv to Fl_{ox} (Bruggeman et al., 1996); the amount of flavin that has to be added to quench the Trp is so large that flavin will absorb part of the excitation light.

Competitive ELISA. Competitive ELISA experiments with anti-Fl_{ox} have been performed using Fl_{ox}, riboflavin and FMN as competitors. We followed the method described by Friguet et al. (1985) except that we did not pre-incubate antibody and antigen. The ELISA plate was coated with a BSA-Flox conjugate, whereas different flavins served as competitive antigens in solution. The results obtained are shown in Table 1 and indicate that the substituent on N10 plays a role in binding: riboflavin and FMN bind worse than Fl_{ox}, to which the antibody was selected. Apparently, the extra phosphate group that FMN possesses compared with riboflavin does not influence binding, neither sterically nor electrostatically.

The same method was used to study binding of anti-Fl_{red} 5 to Fl_{ox} (Bruggeman et al., 1996) and riboflavin. In the latter case we could not determine the apparent binding constant for riboflavin exactly because full inhibition of antibody binding to the ELISA plate by the competing antigen could not be reached. Therefore we conclude that binding to riboflavin is at least several orders of magnitude weaker than to Fl_{ox} (Table 1).

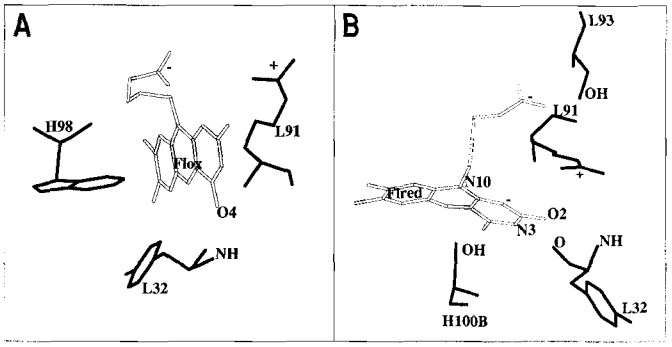

Fig. 6. Fragments of the three-dimensional models of Fl_{ox} bound to anti-Fl_{ox} (A) and of Fl_{red} (deprotonated at N1) bound to anti-Fl_{red} 5 (B), drawn with the graphical program O (Jones et al., 1991).

Redox potentials. Shifts in redox potential ($\Delta E'_0$) values have been calculated for both single-chain Fv fragments for the Fl_{ox}/Fl_{red} couple from the dissociation constants obtained from time-resolved fluorescence data (Table 1) as described by Dutton (1978). For anti-Fl_{ox} we only observe a minor shift, but anti-Fl_{red} 5 causes a 41−65-mV shift in E'_0 dependent on pH. These redox potential shifts indicate that anti-Fl_{ox} binds more to ring A of the flavin or to the N10 substituent and that anti-Fl_{red} is more directed against ring C.

Modelling of the antigen-binding site. To understand the molecular basis of the regulation of the flavin redox potential by the antibody, we took advantage of the highly conserved and well-studied structures of antibody V domains and generated models of the three-dimensional structures of the Fv domains of anti-Fl_{ox} and anti-Fl_{red} 5, based on sequence similarity with antibody structures from the Brookhaven database.

A fragment of the three-dimensional model of the Fl_{ox} · anti-Fl_{ox} complex is shown in Fig. 6A. Fl_{ox} is positioned in a cavity in the anti-Fl_{ox}−binding site that on the bottom side is closed by TrpH47 (±7 Å from ring A of the flavin), while another Trp residue, TrpH50, is much involved in shaping the binding site (TrpH47 and TrpH50 are not shown in this model). These two Trp residues, however, are not directly involved in binding, in contrast to TrpH98. Fl_{ox} is bound mainly by hydrophobic interaction of this residue with ring A of the flavin. The N1/C2=O part of ring C and the main part of the 'tail' (except for the terminal carboxyl group that points back to the protein) stick out of the antigen-binding site into the solvent. There is a hydrogen bond between flavin C4=O and the backbone NH of TyrL32. Another important factor governing the flavin binding is an electrostatic interaction between ArgL91 and the terminal carboxyl group of the flavin N10 substituent (±4 Å).

Fig. 6B shows a fragment of the model of Fl_{red} · anti-Fl_{red} 5 in which N1 is negatively charged. Fl_{red} is well embedded in the antigen-binding site. Ring C of the flavin is bound by two hydrogen bonds: between flavin C2=O and the backbone NH of TyrL32, and between flavin N3H and the backbone C=O of TyrL32. In addition there is a hydrogen bond between flavin N10 and SerH100B. The N10 substituent of the flavin ('tail') plays an important role in binding since the terminal carboxyl group forms a hydrogen bond with SerL93 and a salt bridge with ArgL91 (this is the same residue that is involved in 'tail' binding in anti-Fl_{ox}). This flexible Arg residue can move from the terminal carboxyl group to the negatively charged N1, which explains why negatively charged Fl_{red} is bound more strongly than its neutral form.

Analysis of the hypervariable loops involved in binding revealed that anti-Fl_{ox} uses four CDR (L1, L3, H2 and H3) to bind the flavin. H2 is involved in shaping the binding site but not directly in binding the flavin. The binding site of anti-Fl_{red} 5 is predominantly shaped by L1, L3, H1, H2 and H3, and residues of L1, L3 and H3 are directly involved in binding. According to Wilson and Stanfield (1993) the minimum number of CDR used in binding is four, and H3 and L3 are always used, whereas there is a lack of interaction between L2 and smaller antigens or haptens. Here, we see this absence of L2 in hapten binding for both our antibodies.

The light chain is much involved in binding although the binding sites are differently shaped. ArgL91 and TyrL32 are used for binding in anti-Fl_{ox} as well as in anti-Fl_{red} 5. Since the light chain in both antibodies is the same, this illustrates that not only the primary structure of the V domain determines the structure of the binding site, but also that interaction between both domains is of the utmost importance (Steipe et al., 1992).

DISCUSSION

Comparison of data obtained by experimental mapping methods. Binding of single-chain Fv to different flavins was investigated by competitive ELISA and steady-state and time-resolved fluorescence spectroscopy. These experimental data give an indication of the way flavin is bound to anti-Fl_{ox} and anti-Fl_{red} 5 and serve as a basis to judge the validity of the three-dimensional molecular models. However, discrepancies exist between the dissociation constants obtained using different methods.

The dissociation constant of anti-Fl_{ox} for Fl_{ox} determined from time-resolved fluorescence anisotropy data is about threefold higher than that determined by competitive ELISA. This difference might originate from the equilibrium between antibody and antigen in solution (either Fl_{ox}, riboflavin or FMN) in the ELISA plate being affected by the antigen coated on the surface of the plate (Fl_{ox}). This antigen withdraws part of the antibody from the solution. This might be amplified because anti-Fl_{ox} tends to dimerise, so that not only affinity but also avidity plays a role in binding to the flavin coated to the ELISA plate, resulting in a stronger binding to surface-coated antigen than to antigen in solution. This implies that less antigen is needed to satisfy the antibody in solution, resulting in a lower dissociation constant.

Comparison of steady-state fluorescence-spectroscopy data with data obtained by time-resolved fluorescence and competitive ELISA is impossible due to the interference of photooxidation of Trp in the former experiment. However, the affinity constant of anti-Fl_{ox} for Fl_{ox} is low (in the 10^{-5} M range) and data obtained by the same method can be compared with each other.

After comparison of the binding constants for the different flavins, we can draw the following conclusions. Anti-Fl_{ox} binds Fl_{ox} and Fl_{red} approximately equally well, indicating that either ring A of the flavin nucleus or the N10 substituent is involved in binding, since these parts are the same for Fl_{ox} and Fl_{red} (in contrast to ring C that accepts the electrons and adopts a new electron-density distribution upon reduction). Competitive ELISA experiments with Fl_{ox}, riboflavin and FMN (flavin analogues that only differ in their N10 substituent) reveal that binding to this substituent plays a role (Table 1).

Anti-Fl_{red} binds significantly better to Fl_{red} than to Fl_{ox}, as determined by time-resolved fluorescence spectroscopy (Bruggeman et al., 1996), suggesting that ring C of the flavin is involved in binding. This is supported by the finding that the affinity for Fl_{red} is higher when N1, located in ring C, is deprotonated (Bruggeman et al., 1996). Since riboflavin binds less tightly than Fl_{ox} (Table 1), binding to the N10 substituent must also play a role.

Validity of the models. The three-dimensional model of the anti-Fl_{ox}–binding site is in good agreement with the experimental results. The interaction between ring A of the flavin and TrpH98 is the main interaction causing binding of anti-Fl_{ox} to Fl_{ox} or Fl_{red}, which is in agreement with experimental data. This Trp residue is probably the residue sensitive to photooxidation, which fits our assumption that only one Trp residue is involved in photooxidation, as determined from the breakpoint in the titration curve of the quenching of the Trp fluorescence (Fig. 5). From the slower-decreasing second part of this titration curve we concluded that there are other Trp residues involved in binding that are not sensitive to photooxidation but quench the Trp fluorescence via radiationless energy transfer. We assume that TrpH47 and TrpH50 are the residues involved in this process; they are probably too remote or not well positioned for photooxidation. When flavin is excited (as in time-resolved fluorescence experiments) we noticed quenching of the flavin fluorescence that might be ascribed to TrpH98, TrpH47 and TrpH50, or partly to the hydrogen bond between flavin C4=O and TyrL32 (Ghisla et al., 1974).

The electrostatic interaction between the negatively charged carboxyl group at the terminus of the Fl_{ox} N10 substituent and the positively charged ArgL91 explains the lower affinities for FMN and riboflavin compared with that for Fl_{ox}. The presence of this Arg residue is unexpected since there was no negative charge present in the N10 substituent of the original hapten (instead of the carboxyl group there was a peptide bond linking the hapten to a protein carrier).

The model reveals that the N10 substituent is exposed to the solvent, which explains why riboflavin and FMN are bound equally well. The terminal phosphate group of the N10 substituent of FMN cannot apparently form a salt bridge with ArgL91, probably due to torsional or sterical effects (the distance between N10-phosphate in FMN is larger than that of N10-COO^- in Fl_{ox}; moreover, a phosphate group is more bulky than a carboxyl group). Considering this model, the low affinity of anti-Fl_{ox} for Fl_{ox} is not surprising, since there are few amino acid residues (only TrpH98, ArgL91 and TyrL32) directly involved in binding and the flavin is not well embedded in the antigen-binding site.

The three-dimensional model of anti-Fl_{red} 5 is also in good agreement with the experimental results. As in anti-Fl_{ox} the flavin is partly bound via the carboxyl group at the terminus of the N10 substituent by electrostatic interaction with ArgL91 and by a hydrogen bond to SerL93, which explains why Fl_{ox} is bound better than riboflavin. This positively charged Arg residue is flexible enough to move to N1 of the flavin ring when this atom acquires a negative charge. This is the explanation for the difference in binding between protonated and deprotonated Fl_{red} [changes in conformation cannot be the cause because the geometry of Fl_{red} in both ionization states is not greatly different (Hall et al., 1987a)]. The Arg shift is a matter of induced fit, since anti-Fl_{red} 5 was selected against protonated Fl_{red}.

Furthermore, the isoalloxazine nucleus is bound by three hydrogen bonds: between flavin N10 and SerH100B; between C2=O and TyrL32; and between N3H and TyrL32. These hydrogen bonds [in particular the one to N10 (Moonen et al., 1984a)] and the constraint the binding pocket imposes on Fl_{red} explain the increased fluorescence upon antibody binding, because the rapid interconversions of the multiple, non-planar conformations of reduced flavin are reduced (Ghisla et al., 1974; Visser et al., 1991).

Comparison with other flavoproteins. Anti-Fl_{ox} hardly discriminates between Fl_{ox} and Fl_{red}. The A ring of the flavin is buried in the protein and stabilised by hydrophobic interactions. A comparable situation exists in riboflavin-binding protein (Monaco, 1997), where the A ring is stabilised by hydrophobic interactions, and the C ring has electrostatic interactions with amino acid residues. This results in a 1000-fold higher affinity of the riboflavin-binding protein for the oxidized flavin (Blankenhorn, 1978) and therewith a 90-mV decrease in the redox potential.

From previous studies (see introduction) it is known that binding to the redox-active ring C of the flavin ring predominantly regulates the redox potential. Here we have shown that the antibody anti-Fl_{ox} binding predominantly to ring A, has similar affinities for Fl_{ox} and Fl_{red} and thus barely changes the redox potential. The small change in redox potential (+ 8 mV) might be due to a polarising effect of TrpH98 on ring A of the flavin (Hall, 1987). Ring C of the flavin is mainly exposed to the solvent, which makes anti-Fl_{ox} a 'reversed flavodoxin'. In flavodoxin the flavin, FMN, is situated on a scaffold of loops as in the antigen-binding site of an antibody. However, in flavodoxin, ring A of the flavin sticks out to the solvent instead of ring C.

In anti-Fl_{red} 5 the flavin is much more buried in the protein. The model shows a positively charged Arg residue (L91) that not only shields the negatively charged carboxyl group at the end of the N10 substituent of Fl_{red}, but also interacts with N1 when deprotonated. We assume that these interactions are mainly responsible for different affinities for Fl_{ox} and Fl_{red} and for the 65-mV increase in the redox potential when anti-Fl_{red} 5 binds to deprotonated Fl_{red}. When Fl_{red} is protonated at N1, the affinity for Fl_{red} is lower, which we ascribe mainly to the loss of the favorable electrostatic interaction between N1 and ArgL91.

Positively charged residues in the vicinity of ring C are found to increase the flavin redox potential in flavoproteins (*Lindqvist, 1989*; *Hecht* et al., 1993; Vrielink et al., 1991). For flavodoxin it has been explicitly suggested that in particular the interaction with the flavin N1 nucleus is important for the regulation of the redox potential (Vervoort, 1991); the unfavorable electrostatic interaction between the phosphate dianion and the negatively charged flavohydroquinone has been proposed as a partial explanation for the low redox potential of flavodoxins (Moonen et al., 1984b). For oxidases it has been shown that positively charged residues in the vicinity of N1 contribute to increase the redox potential (see introduction).

The hydrogen bonds to flavin N10, C2=O and N3H probably contribute to the stabilisation of Fl_{red} in the binding pocket by increasing the activation barrier for the transition from the bent to the planar conformation (Moonen et al., 1984a).

In the future these models need to be further verified by mutagenesis studies. This will be a comprehensive study since the redox potential is not only regulated by amino acids having a close contact with the flavin, but also by charged residues at a greater distance of the flavin nucleus (Zhou and Swenson, 1995). In the present study we only judged those residues that were in immediate contact with the flavin.

Conclusion. Our approach, using non-natural flavin-binding proteins to investigate the way a protein environment regulates the flavin redox potential, supports observations on natural flavoproteins. These flavin-binding antibodies ('flavobodies') form tailored protein environments that can be generated against any flavin of interest within a few weeks, even if they are not stable under physiological conditions (Bruggeman et al., 1996). Anti-Fl_{red} 5 shows an 'oxidase-like' redox-potential behaviour, confirming the idea that positively charged residues in the vicinity of N1 increase the redox potential. Furthermore this antibody shows that interaction with the flavin N1 directly influences the redox potential. The results obtained with flavobody anti-Fl_{ox}, a flavin-binding antibody that does not resemble a natural flavoprotein, shows that when ring C of the flavin is not involved in binding, the redox potential is not significantly affected.

We thank Prof. Dr A. Plückthun (Universität Zürich) for his participation in the molecular modeling work, and A. van Hoek for assistance in the time-resolved fluorescence measurements.

REFERENCES

Bastiaens, P. I. H., Mayhew, S. G., O'Nuallain, E. M., van Hoek, A. & Visser, A. J. W. G. (1991) Energy transfer between the flavin chromophores of electron-transferring flavoprotein from *Megasphaera elsdenii* as inferred from time-resolved red-edge and blue-edge fluorescence spectroscopy, *J. Fluorescence 1*, 95–103.

Bastiaens, P. I. H., van Hoek, A., Benen, J. A. E., Brochon, J. C. & Visser, A. J. W. G. (1992a) Conformational dynamics and intersubunit energy transfer in wild type and mutant lipoamide dehydrogenase from *Azotobacter vinelandii*. A multidimensional time-resolved polarized fluorescence study, *Biophys. J. 63*, 839–853.

Bastiaens, P. I. H., van Hoek, A., Wolkers, W. F., Brochon, J. C. & Visser, A. J. W. G. (1992b) Comparison of the dynamical structures of lipoamide dehydrogenase and gluthatione reductase by time-resolved polarized flavin fluorescence, *Biochemistry 31*, 7050–7060.

Bernstein, F. C., Koetzle, T. F., Williams, G. J. B., Meyer, E. F., Brice, M. D., Rodgers, J. R., Kennard, O., Shimanouchi, T. & Tasumi, M. (1977) The protein data bank. A computer based archival file for macromolecular structures, *J. Mol. Biol. 112*, 535–542.

Bird, R. E. (1988) Single-chain antigen-binding proteins, *Science 242*, 423–426.

Blankenhorn, G. (1978) Riboflavin binding in egg-white flavoprotein. The role of tryptophane and tyrosine, *Eur. J. Biochem. 82*, 155–160.

Bruggeman, Y. E., Schoenmakers, R. G., Schots, A., Pap, E. H. W., van Hoek, A., Visser, A. J. W. G. & Hilhorst, R. (1995) Monoclonal antibodies against two electron reduced riboflavin and a quantification of affinity constants for this oxygen-sensitive molecule, *Eur. J. Biochem. 234*, 245–250.

Bruggeman, Y. E., Boogert, A., van Hoek, A., Jones, P. T., Winter, G., Schots, A. & Hilhorst, R. (1996) Phage antibodies against an unstable hapten: oxygen sensitive reduced flavin, *FEBS Lett. 388*, 242–244.

Chothia, C. & Lesk, A. M. (1987) Canonical structures for the hypervariable regions of immunoglobulins, *J. Mol. Biol. 196*, 901–917.

De Bellis, D. & Schwartz, I. (1990) Regulated expression of foreign genes fused to lac: control by glucose levels in growth medium, *Nucleic Acids Res. 18*, 1311.

Dutton, P. L. (1978) Redox potentiometry: determination of midpoint potentials of oxidation-reduction components of biological electron-transfer systems, *Methods Enzymol. 54*, 411–435.

Friguet, B., Chafotte, A. F., Djavadi-Ohaniance, L. & Goldberg, M. E. (1985) Measurements of the true affinity constant in solution of antigen-antibody complexes by enzyme-linked immunosorbent assay, *J. Immunol. Methods 77*, 305–319.

Ghisla, S., Massey, V., Lhoste, J.-M. & Mayhew, S. G. (1974) Fluorescence and optical characteristics of reduced flavins and flavoproteins, *Biochemistry 13*, 589–597.

Ghisla, S. & Massey, V. (1989) Mechanisms of flavoprotein-catalyzed reactions, *Eur. J. Biochem. 181*, 1–17.

Gill, S. C. & von Hippel, P. H. (1989) Calculation of protein extinction coefficients from amino acid sequence data, *Anal. Biochem. 182*, 319–326.

Griffiths, A. D., Malmqvist, M., Marks, J. D., Bye, J. M., Embleton, M., McCafferty, J., Baier, M., Holliger, P., Gorick, B. D., Hughes-Jones, N. C., Hoogenboom, H. R. & Winter, G. (1993) Human anti-self antibodies with high specificity from phage display libraries, *EMBO J. 12*, 725–734.

Griffiths, A. D., Williams, S. C., Hartley, O., Tomlinson, I. A., Waterhouse, P., Crosby, W. L., Kontermann, R. E., Jones, P. T., Low, N. M., Allison, T. J., Prospero, T., Hoogenboom, H. R., Nissim, A., Cox, J. P. L., Harrison, J. L., Zaccolo, M., Gherardi, E. & Winter,

G. (1994) Isolation of high affinity human antibodies directly from large synthetic repertoires, *EMBO J. 13*, 3245–3260.

Hall, L. H. (1987) Further consideration of flavin coenzyme biochemistry afforded by geometry-optimized molecular orbital calculations, *Biochemistry 26*, 7401–7409.

Hall, L. H., Orchard, B. J. & Tripathy, S. K. (1987a) The structure and properties of flavins: molecular orbital study based on totally optimized geometries. I. Molecular geometry investigations, *Int. J. Quantum Chem. 31*, 195–216.

Hall, L. H., Orchard, B. J. & Tripathy, S. K. (1987b) The structure and properties of flavins: molecular orbital study based on totally optimized geometries. II. Molecular orbital structure and electron distribution, *Int. J. Quantum Chem. 31*, 217–242.

Hecht, H. J., Kalisz, H. M., Hendle, J., Schmidt, R. D. & Schomburg, D. (1993) Crystal structure of glucose oxidase from *Aspergillus niger* refined at 2.3 Å resolution, *J. Mol. Biol. 229*, 153–172.

Hochuli, E., Dobeli, H. & Schacher, A. (1987) New metal chelate adsorbents selective for proteins and peptides containing neighbouring histidine residues, *J. Chromatogr. 411*, 177–184.

Hoogenboom, H. R. & Winter, G. (1992) Bypassing immunisation. Human antibodies from synthetic repertoires of germline VH gene segments rearranged *in vitro*, *J. Mol. Biol. 227*, 381–388.

Jones, T. A., Zou, J.-Y., Cowan, S. & Kjelgaard, M. (1991) Improved methods for the building of protein models in electron density maps and the location of errors in these models, *Acta. Cryst. A47*, 110–119.

Kabat, E., Wu, T. T., Reid-Miller, M., Perry, H. M., Gottesman, K. S. & Foeller, C. (1992) *Sequences of proteins of immunological interest*, 5th edn, US Department of Health and Human Services, Bethesda.

Knappik, A. & Plückthun, A. (1995) Engineered turns of a recombinant antibody improve its *in vivo* folding, *Protein Eng. 8*, 81–89.

Lindqvist, Y. (1989) Refined structure of spinach glycolate oxidase at 2 Å resolution, *J. Mol. Biol. 209*, 151–166.

Marks, J. D., Hoogenboom, H. R., Bonnert, T. P., McCafferty, J., Griffiths, A. D. & Winter, G. (1991) Bypassing immunization. Human antibodies from V-gene libraries displayed on phage, *J. Mol. Biol. 222*, 581–597.

Monaco, H. L. (1997) Crystal structure of chicken riboflavin-binding protein, *EMBO J. 16* 1475–1483.

Moonen, C. T. W., Vervoort, J. & Müller, F. (1984a) A carbon-13 nuclear magnetic resonance study on the dynamics of the conformation of reduced flavin, *Biochemistry 23*, 4859–4867.

Moonen, C. T. W., Vervoort, J. & Mueller, F. (1984b) Some new ideas about the possible regulation of redox potentials in flavoproteins with special reference to flavodoxins, in *Flavins and flavoproteins* (Bray, R. C., Engel, P. C. & Mayhew, S. G., eds) pp. 493–496, de Gruyter, Berlin.

Munro, S. & Pelham, H. R. B. (1986) An Hsp-like protein in the ER: identity with the 78 kD glucose regulated protein and immunoglobulin heavy chain binding protein, *Cell 46*, 291–300.

Nissim, A., Hoogenboom, H. R., Tomlinson, I. A., Flynn, G., Midgley, C., Lane, D. & Winter, G. (1994) Antibody fragments from a 'single pot' phage display library as immunochemical reagents, *EMBO J. 13*, 692–698.

Perisic, O., Webb, P. A., Holliger, P., Winter, G. & Williams, R. L. (1994) Crystal structure of a diabody, a bivalent antibody fragment, *Structure (Lond.) 2*, 1217–1226.

Platenkamp, R. J., Palmer, M. H. & Visser, A. J. W. G. (1987) *Ab initio* molecular orbital studies of closed shell flavins, *Eur. Biophys. J. 14*, 393–402.

Shokat, K., Leumann, C. H., Sugasawara, R. & Schultz, P. G. (1988) *Eine über Antikorper gesteuerte Redoxreaktion*, *Angew. Chem. 100*, 1227–1229.

Stankovich, M. T. (1990) Redox properties of flavins and flavoproteins, in *Chemistry and biochemistry of flavoenzymes* (Müller, F., ed.) vol. 1, pp. 401–425, CRC Press, Boca Raton.

Steipe, B., Plückthun, A. & Huber, R. (1992) Refined crystal structure of a recombinant immunoglobulin domain and a complementarity-determining region 1-grafted mutant, *J. Mol. Biol. 225*, 739–753.

Taylor, M. B. & Radda, G. K. (1971) Flavins as photosensitizers, *Methods Enzymol. 18B*, 496–506.

Tomlinson, I. A., Walter, G., Marks, J. D., Llewelyn, M. B. & Winter, G. (1992) The repetoire of human germline V_H sequences reveals about fifty groups of V_H segments with different hypervariable loops, *J. Mol. Biol. 227*, 776–797.

Vervoort, J. (1991) Electron-transferring proteins, *Curr. Opin. Struct. Biol. 1*, 889–894.

Visser, A. J. W. G., Ghisla, S. & Lee, J. (1991) Picosecond fluorescence dynamics of reduced flavins, in: *Flavins and flavoproteins 1990* (Curti, B., Ronchi, S. & Zanetti, G., eds) pp. 49–54, de Gruyter, New York.

Vrielink, A., Lloyd, L. & Blow, D. M. (1991) Crystal structure of cholesterol oxidase from *Brevibacterium sterolicum* refined at 1.8 Å resolution, *J. Mol. Biol. 219*, 533–554.

Wilson, A. & Stanfield, R. L. (1993) Antibody-antigen interactions, *Curr. Opin. Struct. Biol. 3*, 113–118.

Zhou, Z. & Swenson, R. P. (1995) Electrostatic effects of surface acidic amino acid residues on the oxidation-reduction potentials of the flavodoxin from *Desulfovibrio vulgaris* (Hildenborough), *Biochemistry 34*, 3183–3194.